Brillouin fiber optic gyro with push-pull phase modulator and synthetic heterodyne detection

S. Huang, K. Toyama, P.-A. Nicati, L. Thévenaz, B. Y. Kim, H. J. Shaw

Edward L. Ginzton Laboratory
Stanford University, Stanford, CA 94305

ABSTRACT

Intracavity phase modulation in a fiber optic ring laser gyro can provide "optical dithering" to reduce the effects of frequency locking while retaining optical reciprocity in the cavity. We show that the use of two antiphased phase modulators placed symmetrically within the fiber cavity can provide uniformly distributed dithering. A modulation index of 2.4 theoretically eliminates the zero-order lock-in band around zero frequency, while use of a high modulation frequency puts higher-order lock-in bands outside the beat frequency dynamic range. Push-pull modulation allows for high modulation frequency with minimum dynamic perturbation of the cavity resonant behavior. We describe results with an experimental Brillouin fiber optic gyro operating at 1.3 μm wavelength using push-pull modulation together with a novel synthetic heterodyne detection scheme for sensing rotation rate and direction. A ten-fold reduction of the width of the zero-order lock-in band is observed. We also demonstrate that the observed frequency bias at zero rotation rate is caused by Kerr effect due to power imbalance between the two oppositely directed circulating lasers.

1. INTRODUCTION

When the rotation rate of a ring laser gyro is below the so-called lock-in threshold, the frequencies of the two counterpropagating waves in the resonant cavity are locked to a common value.[1] Thus, the ring laser gyro is not responsive within a region of small rotation rate, which brings about a dead band at the center of the rotation dynamic range.

The usual methods for the avoidance of lock-in are to introduce a constant frequency bias[2,3] or alternating frequency bias[4] between the two waves so that the beat frequency of the two lasers can be brought outside the lock-in range. A difficulty with the former is that the constant bias has to be a large number known with high accuracy, and the reciprocity would be actually broken if the constant bias is introduced by exciting different longitudinal modes in the laser cavity. Therefore, the latter method is more acceptable. Mechanical "dithering" was the most successful alternating-bias technique. But, an optical approach which does not need a body dithering and still maintains the optical reciprocity is more attractive.

A scheme of optical dithering by a push-pull intracavity phase modulation was used in a ring laser gyro.[5] The phase modulation was implemented through a vibrating-prism biasing device in the cavity, which shows some difficulties in applications for both mechanism and optics. In this paper, we describe a fiber-optic Brillouin ring laser gyro with push-pull modulation by using two optical-fiber phase modulators. This in-line modulation allows a simple system with very easy dither controlling. Similar technique has been reported to apply to a fiber laser linear-cavity for suppressing spatial hole burning.[6]

2. SUPPRESSION OF LOCK-IN

2.1. Principle

 0-8194-0974-X/93/$4.00

The directional characteristic of stimulated Brillouin scattering makes a fiberoptic resonator capable of supporting two independent counterpropagating lasers, by pumping in both directions.[2,3] In order to calculate the effect of an intracavity phase modulation on the two lasers, we consider a Brillouin fiberoptic ring cavity, with two phase modulators (PMs) driven by $\phi_{m,1}(t)$ and $\phi_{m,2}(t)$ respectively, shown in figure 1. The two modulators divide the ring into two parts, I and II, with lengths of l_1 and l_2 respectively (the ring perimeter $l = l_1 + l_2$). The quasi static analysis[7] can be employed here as long as the modulation period is fairly longer than one round-trip transit time of the light, T.

Let $\phi_1(t, z_1)$ denote the quasi-static incremental phase due to the modulation, at a point Q_1 in region I with a displacement of z_1 from PM1. Similarly, we define $\phi_2(t, z_2)$ for a point Q_2 in region II with a displacement of z_2 from PM2, as shown in Fig. 1. For the clockwise and counterclockwise laser waves, we have

$$\begin{cases} \phi_1^{(cw)}\left(t-\dfrac{l_1-z_1}{l}T, z_1\right)+\phi_{m,2}(t)=\phi_2^{(cw)}\left(t+\dfrac{z_2}{l}T, z_2\right) \\ \phi_2^{(cw)}\left(t-\dfrac{l_2-z_2}{l}T, z_2\right)+\phi_{m,1}(t)=\phi_1^{(cw)}\left(t+\dfrac{z_1}{l}T, z_1\right) \end{cases} \tag{1}$$

and

$$\begin{cases} \phi_1^{(ccw)}\left(t-\dfrac{z_1}{l}T, z_1\right)+\phi_{m,1}(t)=\phi_2^{(ccw)}\left(t+\dfrac{l_2-z_2}{l}T, z_2\right) \\ \phi_2^{(ccw)}\left(t-\dfrac{z_2}{l}T, z_2\right)+\phi_{m,2}(t)=\phi_1^{(ccw)}\left(t+\dfrac{l_1-z_1}{l}T, z_1\right) \end{cases} \tag{2}$$

respectively. The two PMs are essentially required to operate in push-pull manner so as to minimize the dynamic perturbation of the cavity resonant behavior. For a sinusoidal push-pull modulation, i. e. $\phi_{m,1}(t) = -\phi_{m,2}(t) = \Phi_m \sin\omega_m t$, we can readily solve all quasi-static phases from Eq.(1) and Eq.(2). In consequence, the modulation-induced differential instantaneous frequencies between the two counterpropagating lasers, at Q_1 and Q_2, can be obtained as

$$\begin{aligned} \Delta\omega(t, z_1) &= \frac{d}{dt}[\phi_1^{(cw)}(t, z_1) - \phi_1^{(ccw)}(t, z_1)] \\ &= 2\Phi_m\omega_m \frac{\sin\left(\omega_m \dfrac{l_2}{2l}T\right)\cos\left(\omega_m \dfrac{l_1-2z_1}{2l}T\right)}{\sin(\omega_m T/2)}\cos\omega_m t \end{aligned} \tag{3a}$$

and

$$\begin{aligned} \Delta\omega(t, z_2) &= \frac{d}{dt}[\phi_2^{(cw)}(t, z_2) - \phi_2^{(ccw)}(t, z_2)] \\ &= -2\Phi_m\omega_m \frac{\sin\left(\omega_m \dfrac{l_1}{2l}T\right)\cos\left(\omega_m \dfrac{l_2-2z_2}{2l}T\right)}{\sin(\omega_m T/2)}\cos\omega_m t \end{aligned} \tag{3b}$$

respectively. It can be seen from Eqs. (3a) and (3b) that an alternating frequency bias between the two laser oscillators (i. e. an optical dither) has been produced by the modulation. The amplitude of the alternating bias (i. e. the dither depth) is

generally position-dependent. But, if the two PMs are placed symmetrically in the cavity ring, i. e. $l_1 = l_2 = l/2$, a position-independent dither depth will be obtained with

$$\Delta\omega(t, z_1) = -\Delta\omega(t, z_2) \approx \Phi_m \omega_m \cos\omega_m t \tag{4}$$

provided that the quasi-static condition, $\omega_m T << 2\pi$, is satisfied. In view of the fact that a fiberoptic ring has randomly distributed backscattering in addition to the backscattering from the coupler and the fiber splice, a dither with 'uniform' depth along the ring cavity is supposed to be more effective to suppress frequency locking. It should be mentioned that the dithers in region I and region II are antiphased, though they have the same depth.

2.2. Description of Brillouin ring laser gyro

An all-fiber (non-PM fiber) Brillouin ring laser gyro with push-pull modulation has been set up. Its schematic diagram is shown in figure 2. This gyro consists of three fused-type directional couplers which are made by non-PM single-mode optical fiber at 1.3 μm (Corning, SMF-28). Coupler C1 splits the input pump power into two nominally equal parts; while coupler C2 and coupler C3 have weak power coupling (~a few percent). A laser-diode pumped ring Nd:YAG laser at wavelength of 1.32 μm (made by Lightwave Electronics) is used as the pump light source. The resonator cavity is locked to the pump frequency by a stabilization circuit, so that the highest circulating pump-power level can be attained in the cavity. Above the pumping threshold, two counterpropagating Brillouin laser waves, oppositely-directed to their pumps, are generated in the cavity and coupled out through C2. Coupler C3 taps out a portion of pump P1 downstream from the cavity and feeds it to the stabilization circuit.

Two PZT phase modulators in push-pull manner are symmetrically located in the cavity. The coil diameter is ~20 cm, and the total cavity length is ~27 m including the parts wound on the two PZTs, which gives a free spectrum range of ~7.6 MHz. In order to produce a phase modulation for the purpose of stabilization, we can either use an additional PZT phase modulator at the input port (PM3 in Fig. 2), or just simply make use of the existing 'residual' cavity modulation due to the transit time delay under push-pull modulation.

Two polarization controllers, PC1 and PC2, are placed in the fiber external circuit to make the two pump waves be in the same eigen-polarization mode in the resonator cavity. Via C1, the two output Brillouin waves combine and produce a beat note at detector D_1. The beat frequency gives the gyro rotation rate. Because of reciprocity, little pump power is received at D_1 as long as the two pumps excite the same eigen-polarization mode in the cavity and well balanced in power. This is advantageous for minimizing shot noise without requiring a pump filter ahead of D_1. This condition also provides a simple means for the adjustment of PC1 which can not be monitored directly.

2.3. Selection of modulation index and frequency

The lock-in reduction depends on the amplitude and frequency of the push-pull modulation signal. In this section, we discuss the selection of the modulation index and modulation frequency for the sinusoidal modulation case, in which an alternating frequency bias of $\pm\Phi_m\omega_m\cos\omega_m t$ is obtained (see Eq.(4)).

The final output signal of the ring laser gyro with sinusoidal push-pull modulation, received by detector D_1, is

$$I(t) = \frac{I_0}{2}\left\{1 + \cos\left[\int_0^t (\pm\Phi_m\omega_m\cos\omega_m t + \Omega_b)dt\right]\right\}$$
$$= \frac{I_0}{2}[1 + \cos(\pm\Phi_m \sin\omega_m t + \Omega_b t + \phi_0)]$$

$$= \frac{I_0}{2}\{1 + J_0(\Phi_m)\cos(\Omega_b t + \phi_0)$$
$$\pm J_1(\Phi_m)[\cos((\omega_m + \Omega_b)t + \phi_0) - \cos((\omega_m - \Omega_b)t - \phi_0)]$$
$$+ J_2(\Phi_m)[\cos((2\omega_m + \Omega_b)t + \phi_0) + \cos((2\omega_m - \Omega_b)t - \phi_0)]$$
$$\pm J_3(\Phi_m)[\cos((3\omega_m + \Omega_b)t + \phi_0) - \cos((3\omega_m - \Omega_b)t - \phi_0)]$$
$$+ \ldots\ldots\} \quad (5)$$

where $I_0/2$ is the intensity of each output Brillouin wave, Ω_b is the rotation-induced beat frequency, ϕ_0 is the initial phase, and J_n denotes the nth-order Bessel function. In accordance with the sign convention for beat frequency used in Eqs. (3a) and (3b), positive Ω_b and negative Ω_b respectively correspond to counterclockwise (CCW) and clockwise (CW) rotation directions. The sign selection of '+' or '-' in Eq. (5) is determined by that the coupler C2 is located in region I or region II.

With this sinusoidal 'dither', a new lock-in distribution picture will replace the one which occurs without dither. We will obtain a series of dead-bands instead of the only central dead-band.[8] These dead bands correspond to the rotation rates $\Omega_b = \pm n\omega_m$ with widths proportional to $|J_n(\Phi_m)|$, where n = 0, 1, 2, ... It can be seen that the central dead-band will vanish if Φ_m is chosen to be 2.4 rad. Therefore a good linear response of beat-frequencies to rotation rates can be obtained within the required rotation dynamic range as long as Φ_m = 2.4 rad and also $f_m = \omega_m/2\pi$ is high enough such that the first-order dead-band is placed outside the rotation dynamic range. For example, if the scale factor of the gyro is 1 kHz/(deg/sec), the f_m should be larger than 300 kHz to bring the first dead-band beyond the maximum rotation rate of 300 deg/sec. With this value of f_m, the quasi-static condition is still satisfied if we take a typical fiber-cavity length of $l \sim 20$ m, and hence a transit time of $T \sim 0.1$ μs.

Figure 3 shows the frequency spectra of $I(t)$ for both rotation directions, $\Omega_b > 0$ and $\Omega_b < 0$. Note that Fig. 3 corresponds to the case of that the coupler C2 is located in region I, i. e. the sign '+' is taken in Eq. (5). Since there is no longer the DC sideband in the case of Φ_m = 2.4 rad, the rotation beat frequency Ω_b will be read at the harmonics, which is advantageous for reducing electronic noise.

2.4. Experiments

The lock-in reduction through push-pull phase modulation has been tested at our Brillouin ring laser gyro. The final output signal is monitored by a HP35665 Dynamic Signal Analyzer in frequency and/or time domain. Figure 4(a) gives the lowest beat frequency observed, of ~ 500 Hz, in the absence of push-pull modulation. The poor spectrum and distorted time-domain signal indicate the beginning of lock-in. After applying push-pull modulation to the cavity, a ~50 Hz rotation-induced beat frequency could be measured which showed a lock-in reduction by factor of 10. The modulation frequency used was f_m = 11 kHz and the modulation index was Φ_m = 2.4 rad. Figure 4(b) shows the ~50 Hz beat frequency read at the first harmonic (11 kHz). Reduction of lock-in has been also observed under higher modulation frequencies. But, adjusting the amplitude balance and antiphase for the push-pull was found quite critical, and more difficult under high modulation frequencies. Under a high modulation frequency f_m, the 'dynamic response' problem may occur,[9] although it has been relieved to a great extent in the push-pull scheme in comparison with a single-modulator case. Once a cavity is modulated with high frequency or high index, the superposed components from different trips in the resonator would see different cavity lengths, hence different phase delays. As the result, the average circulating pump power would be reduced and therefore the pumping efficiency would be reduced. With all real parameters of our gyro system, we have calculated the normalized circulating pump power in the ring cavity under a sinusoidal push-pull modulation with Φ_m = 2.4 rad. The calculation shows that the pumping efficiencies at f_m = 20 kHz, 100 kHz, and 1 MHz would be reduced to 89%, 52% and 38% of that at f_m = 1 kHz, respectively.

3. SYNTHETIC HETERODYNE DETECTION

3.1. Sensing rotation direction

From the beat note output of a ring laser gyro, one can obtain the gyro rotation rate but not the rotation sense. One type of readout which can sense both rotation rate and direction is spatial quadrature detection.[1,8] For a fiberoptic ring laser gyro, however, this method seems not appealing. In order to get spatial quadrature signals, we have to extract both lasers through optical fiber couplers before the two lasers combine, and then obtain the interference pattern of the two sampled laser-beams by using some bulk optics components.

For fiberoptic ring laser gyros, the scheme[2,3] with a large constant frequency bias between the two counterpropagating lasers can easily sense rotation direction by checking whether the measured beat frequency is larger or smaller than the bias. However, as mentioned before, this scheme itself may have difficulties with reciprocity and stability. Here we investigate the ring laser gyro with sinusoidal phase modulation, in which an ac-bias is introduced. In the same principle as the dc-bias case, this 'known' ac-bias should be also able to serve as a reference for judging rotation direction as long as we synchronize the readout with the modulation driving-signal.

3.2. Theory

Generally speaking, according to Eqs. (1) and (2), using only one phase-modulator in the ring cavity is enough to produce an ac-bias between the two counterpropagating lasers, the amplitude of which is position-dependent. However, considering the practical applications, we discuss here only the ring cavity having two symmetrically-located modulators with sinusoidal push-pull phase modulation. Therefore, all results in Section 2 can be used in this discussion.

From Fig. 3, it is clear that the spectra of the gyro output signal $I(t)$ are different for $\Omega_b > 0$ and $\Omega_b < 0$. When $\Omega_b > 0$, the right sidebands of all harmonics, i. e. $n\omega_m+\Omega_b$ (n=1, 2, 3,..), have the same sign; while the left sidebands, i. e. $n\omega_m-\Omega_b$ (n=1, 2, 3,..), change signs alternately (see Fig. 3). But, when $\Omega_b < 0$, the situation for right and left sidebands is reversed. Based on these spectral characteristics, we propose a simple synthetic heterodyne detection scheme to sense both rotation rate and direction. This is related to an approach used with interferometric gyros.[10]

The synthetic heterodyne signal processing circuit is shown in figure 5. The output of the ring laser gyro, $I(t)$ (see Eq. (5)), is AC-coupled to a mixer. Through the mixer, the AC part of $I(t)$ is multiplied by a signal $A(t) = A(\alpha+\cos\omega_m t)$ where ω_m is the push-pull modulation frequency, and A is an arbitrary real number. The DC weight, α, is chosen to be 0.4158 while the push-pull modulation index Φ_m = 2.4 rad, so that $\alpha J_1(2.4) - 1/2\, J_2(2.4) = 0$. Then the output of the mixer, $S(t)$, can be obtained as

$$S(t) = \frac{I_0}{2}\{0.4318\cos((\omega_m + \Omega_b)t + \phi_0) + \text{other harmonics}\}. \quad (6)$$

It can be seen from Eq. (6) that the sideband at $\omega_m-\Omega_b$ is absent after the processing. The remaining single sideband $\omega_m+\Omega_b$, shown in Fig. 5, can be easily picked up by a band-pass filter around ω_m. One can see that the location of this single sideband gives the rotation rate and sense at the same time. This location, i. e. the frequency readout after the processing, f_{ro}, is very easy to measure by means of a spectrum analyzer or a frequency counter.

3.3. Experiments

This scheme has been tested with our Brillouin fiberoptic ring laser gyro. The push-pull modulation frequency and index used were f_m = 11 kHz and Φ_m = 2.4 rad respectively. Note that whether CW rotation (or CCW rotation) corresponds to a

right sideband ($f_{ro}>f_m$) or a left sideband ($f_{ro}<f_m$) is determined by two factors. First, this depends on which region of the cavity the coupler C2 is located in. If coupler C2 is located in region II instead of region I (equivalent to interchanging the modulation signals on the two PMs), the spectrum pictures in Fig. 3 and Fig. 5 will change. All left and right sidebands will exchange each other. Second, if the phase delay in the $A(t)$ generator (Fig. 5) is shifted by 180°, we will have $A(t) = A(\alpha - \cos\omega_m t)$ instead of $A(t) = A(\alpha+\cos\omega_m t)$. Then the surviving single sideband will be $\omega_m-\Omega_b$ instead of $\omega_m+\Omega_b$, and hence the spectra of $\Omega_b > 0$ and $\Omega_b < 0$ in Fig. 5 will be interchanged. Therefore, under different conditionts, CW and CCW rotations can show reversed remaining sideband.

Two measured curves of readout frequency f_{ro} vs rotation rate Ω_b are given in figure 6. These two curves are of good linearity, but with opposite slopes because they correspond to phase delays, in the $A(t)$ generator of Fig. 5, having a 180° difference.

4. KERR-EFFECT-INDUCED BIAS

As can be seen from Fig. 6, the readout frequency at zero rotation is not 11 kHz; instead, there is a positive or negative frequency bias depending on the curve slope. It has been found that this bias is induced by Kerr-effect due to a power imbalance between the two counterpropagating lasers in the resonant cavity.

In our present system, the two pumps fed into the ring cavity are quite unbalanced because the coupler C1 has an imperfect splitting ratio (~0.54/0.46) for the two beams and then the weaker beam is further tapped by coupler C3. Thus in the cavity, the CCW pump circulating-power is stronger than the CW pump, and hence the CW Brillouin circulating-power is stronger than the CCW Brillouin wave. Because of the Kerr-effect perturbation on the refractive index, the stronger Brillouin wave (CW) receives a larger Kerr-effect-induced increment on the refractive index and therefore sees a longer optical path, than the CCW Brillouin wave. As the result, a nonreciprocity due to Kerr-effect is induced in the present system, which is equivalent to the nonreciprocity introduced by a CCW gyro rotation. One can see from Fig. 6 that both curves show a shift towards the CCW rotation direction.

In order to verify this Kerr-effect-induced bias, we introduced a loss into the stronger pump beam by bending the external fiber arm such that the pumping imbalance becomes adjustable. With the differential pump power from positive to zero and then to negative, the beat frequency at zero rotation rate shows a bias from CCW-rotation-oriented to zero, and then to CW-rotation-oriented. The research details on Kerr-effect in the Brillouin ring laser gyro are to be published elsewhere.

5. CONCLUSION

A ten-fold reduction of the lock-in range has been demonstrated in a fiberoptic Brillouin ring laser gyro which utilizes a push-pull phase modulation in the ring cavity. This rugged in-line gyro system reduces lock-in without breaking optical reciprocity in the cavity. As a compatible scheme with the sinusoidal push-pull phase modulation technique, a synthetic heterodyne detection method for ring laser gyro to sense both rotation rate and direction is also demonstrated. In this detection, only a simple signal processing is needed. Further suppressing the lock-in range and reducing the Kerr-effect-induced beat frequency bias are our next aims.

This research was supported by Litton Systems, Inc.

6. REFERENCES

1. F. Aronowitz, *laser Applications*, Vol. 1, Academic, New York, 1971, p. 148

2. R. K. Kadiwar and I. P. Giles, "Optical fiber Brillouin ring laser gyroscope," *Electron. Lett.*, Vol. 25, pp. 1729-1731, Dec. 1989.

3. F. Zarinetchi, S. P. Smith, and S. Ezekiel, "Stimulated Brillouin fiber-optic laser gyroscope," *Opt. Lett.*, Vol. 16, pp. 229-231, Feb. 1991.

4. T. J. Hutchings and D. C. Stjern, "Scale factor non-linearity of a body dither laser gyro," *Proc. IEEE National Aerospace Electronic Conf.*, IEEE, New York, 1978, pp. 549-555.

5. H. A. H. Boot, P. G. R. King, and R. B. R. Shersby-Harvie, "Ring-laser bias using reciprocal optical components," *Electron. Lett.*, Vol. 5, pp. 347-348, July 1969.

6. H. Sabert and R. Ulrich, "Spatial hole burning in Nd^{3+}-fiber lasers suppressed by push-pull phase modulation," *Appl. Phys. Lett.*, Vol. 58, pp. 2323-2325, May 1991.

7. A. E. Siegman, *lasers*, University Science Books, Mill Valley, Calif., 1986, p. 982

8. W. W. Chow, J. Gea-Banacloche, L. M. Pedrotti, V. E. Sanders, W. Schleich, and M. O. Scully, "The ring laser gyro," *Rev. Modern Physics*, Vol. 57, pp. 61-104, Jan. 1985.

9. Z. K. Ioannidis, P. M. Radmore, and I. P. Giles, "Dynamic response of an all-fiber ring resonator," *Opt. Lett.*, Vol. 13, pp. 422-424, May 1988.

10. B. Y. Kim and H. J. Shaw, "Phase-reading, all-fiber-optic gyroscope," *Opt. Lett.*, Vol. 9, pp. 378-380, Aug. 1984.

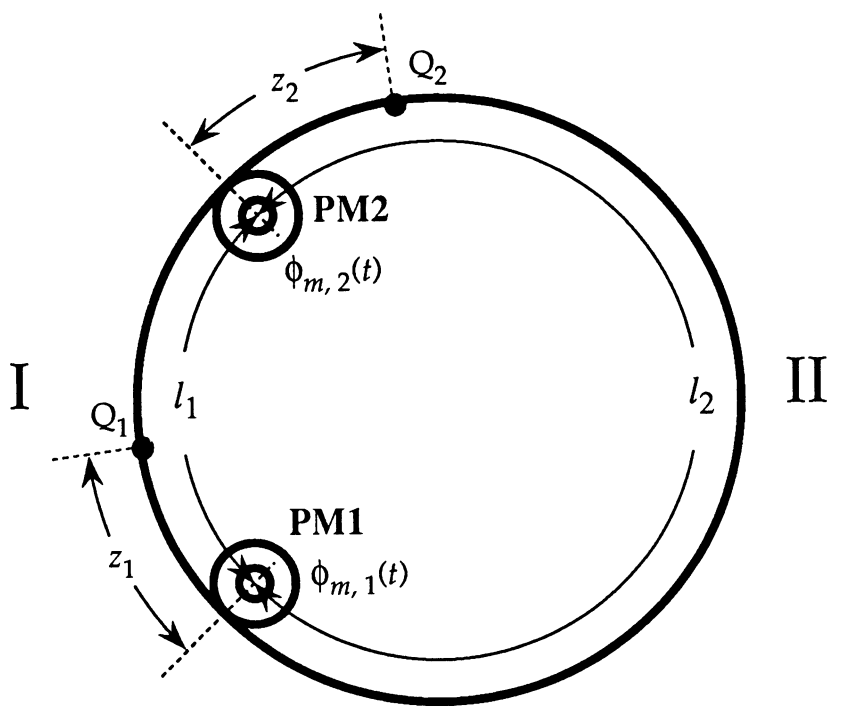

Figure 1. Fiberoptic ring cavity with two phase modulators (PMs).

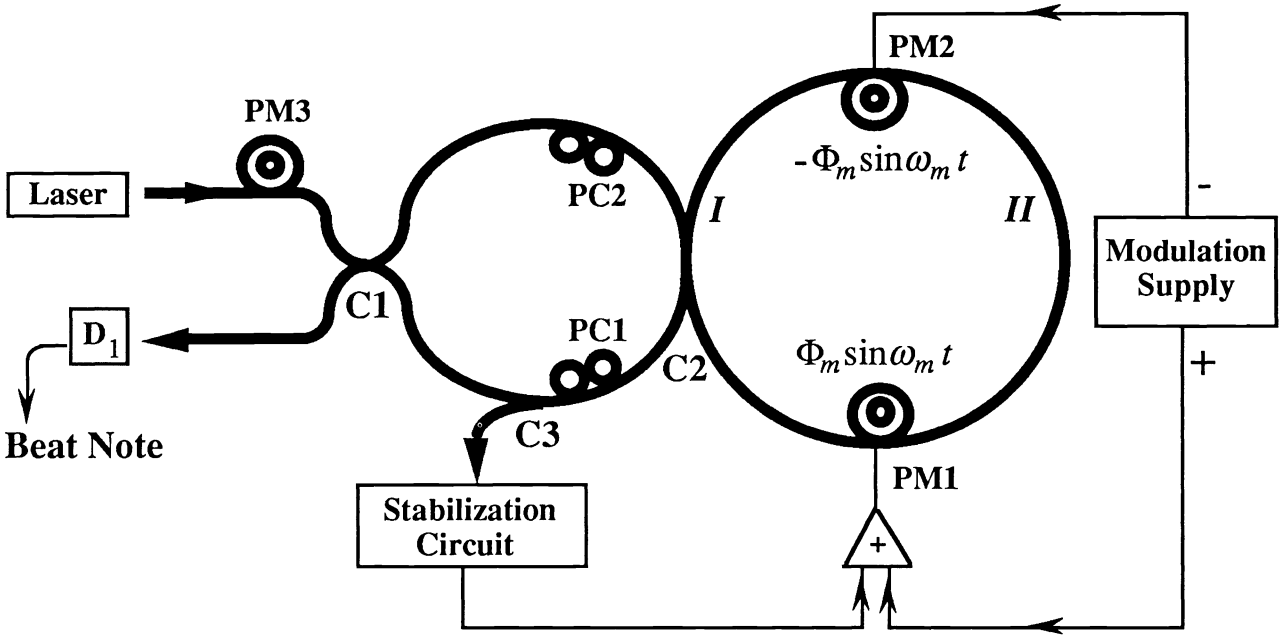

Figure 2. Experimental setup: PM, phase modulator; PC, polarization controller; C, optical-fiber coupler; D, detector.

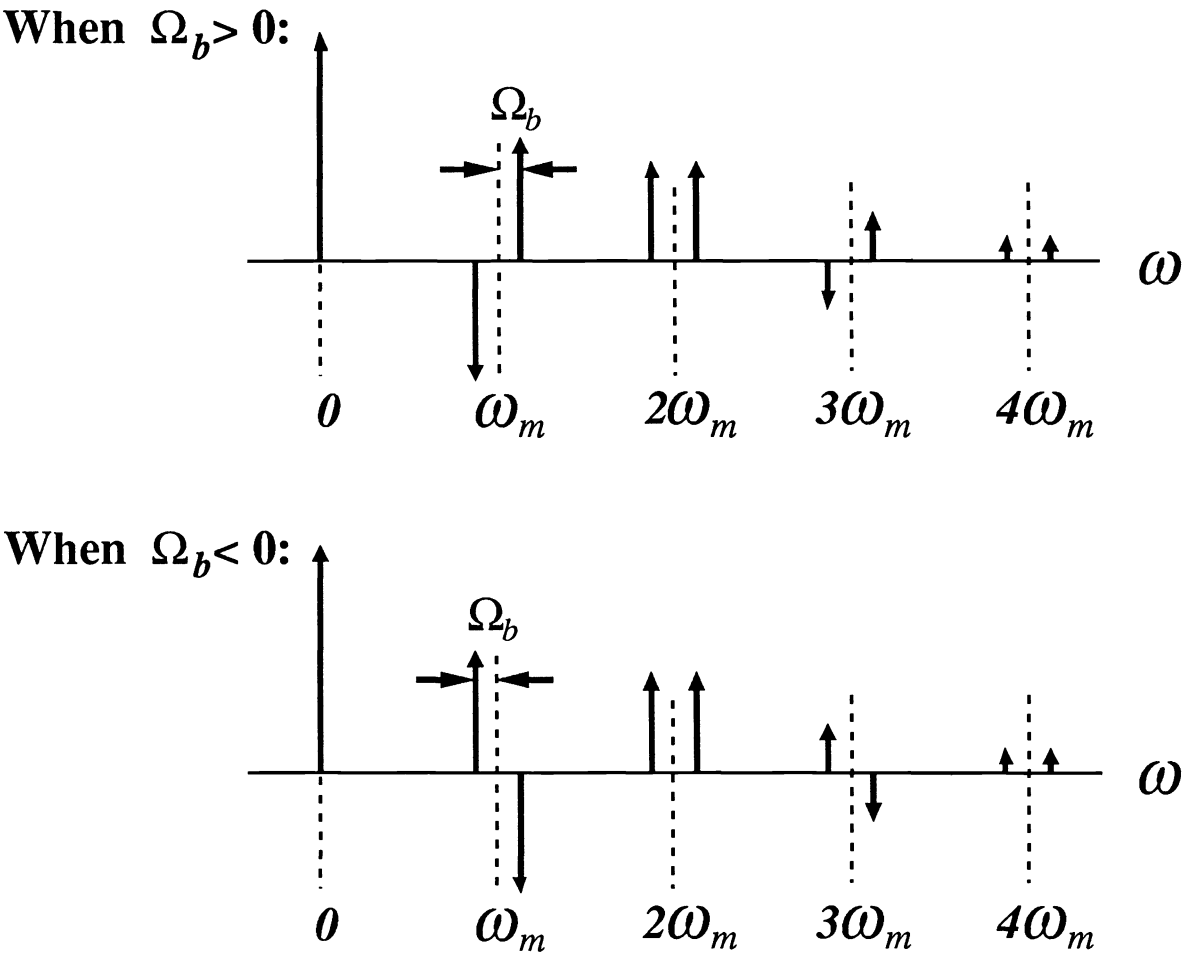

Figure 3. Frequency spectra of the final output signals from the gyro, for two opposite rotation directions, when $\Phi_m = 2.4$ rad and the coupler C2 is in region I (see Fig. 2).

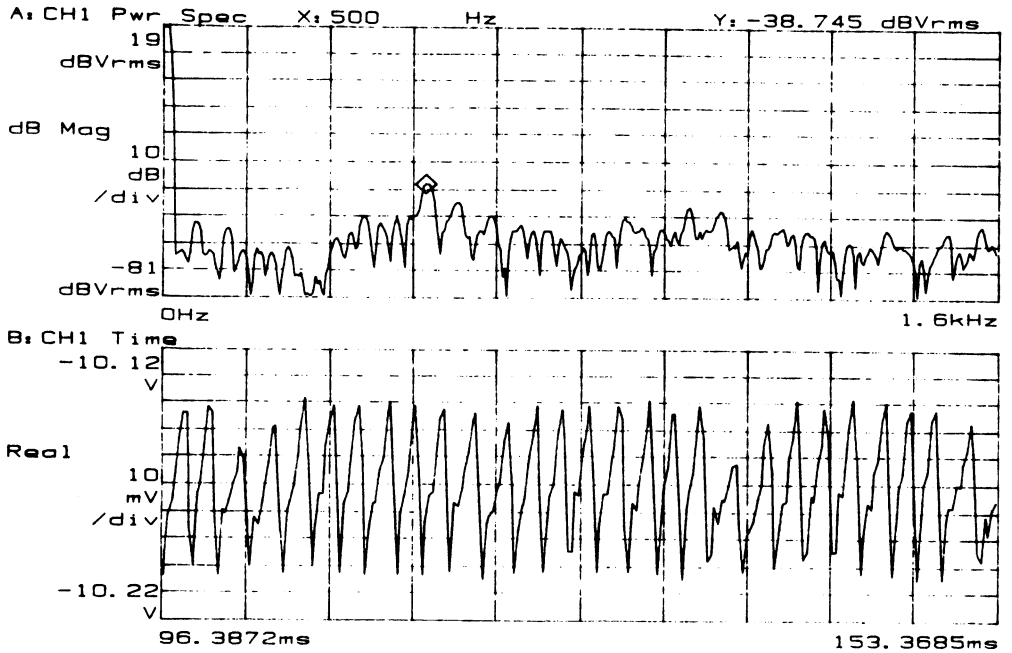

(a)

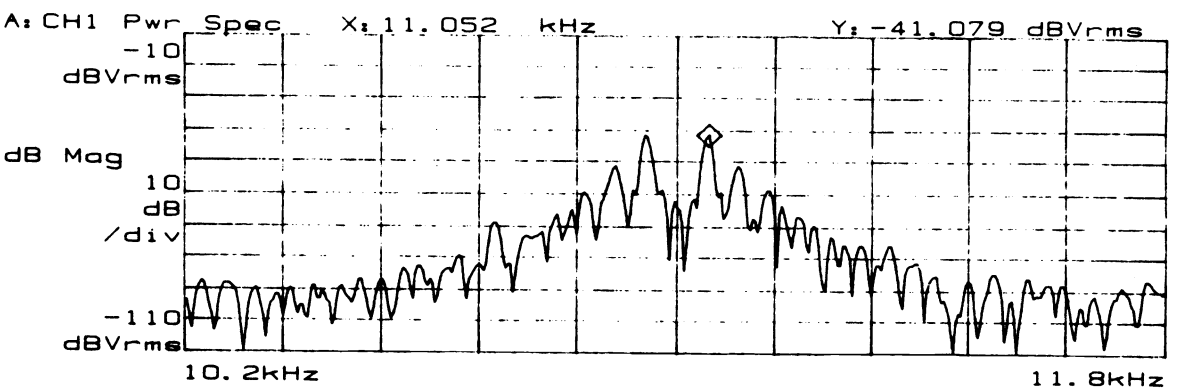

(b)

Figure 4. (a) Measured output signal in frequency domain (upper) and time domain (lower) without modulation. Measured beat frequency = 500 Hz; the time-domain signal is distorted indicating an on-set of lock-in.
(b) Measured output signal in frequency domain around the first-harmonic with push-pull modulation frequency of 11 kHz. Measured beat frequency = 52 Hz, shifted by the modulation frequency of 11 kHz.

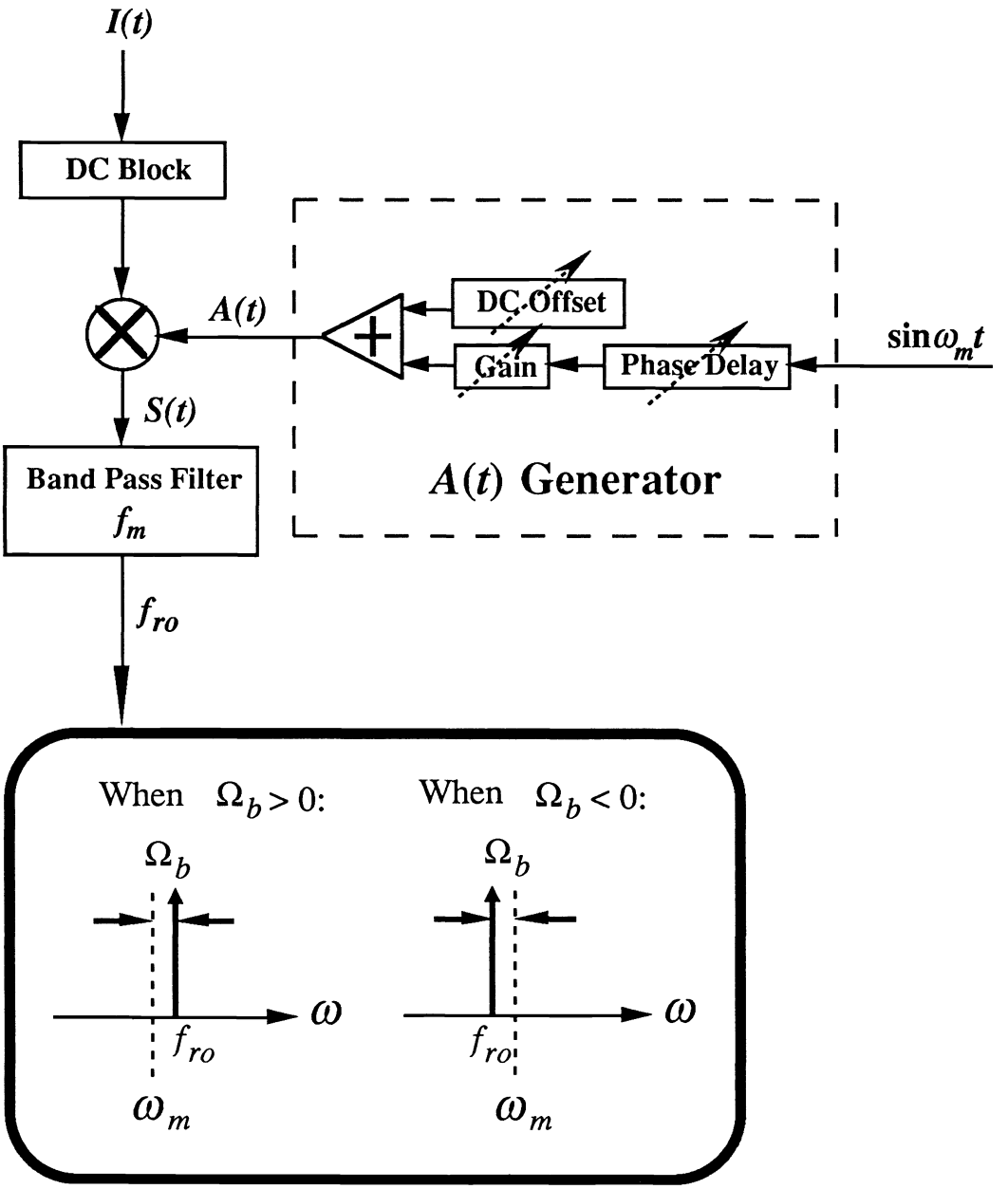

Figure 5. Synthetic heterodyne signal processing circuit, and the frequency spectra of the output signal.

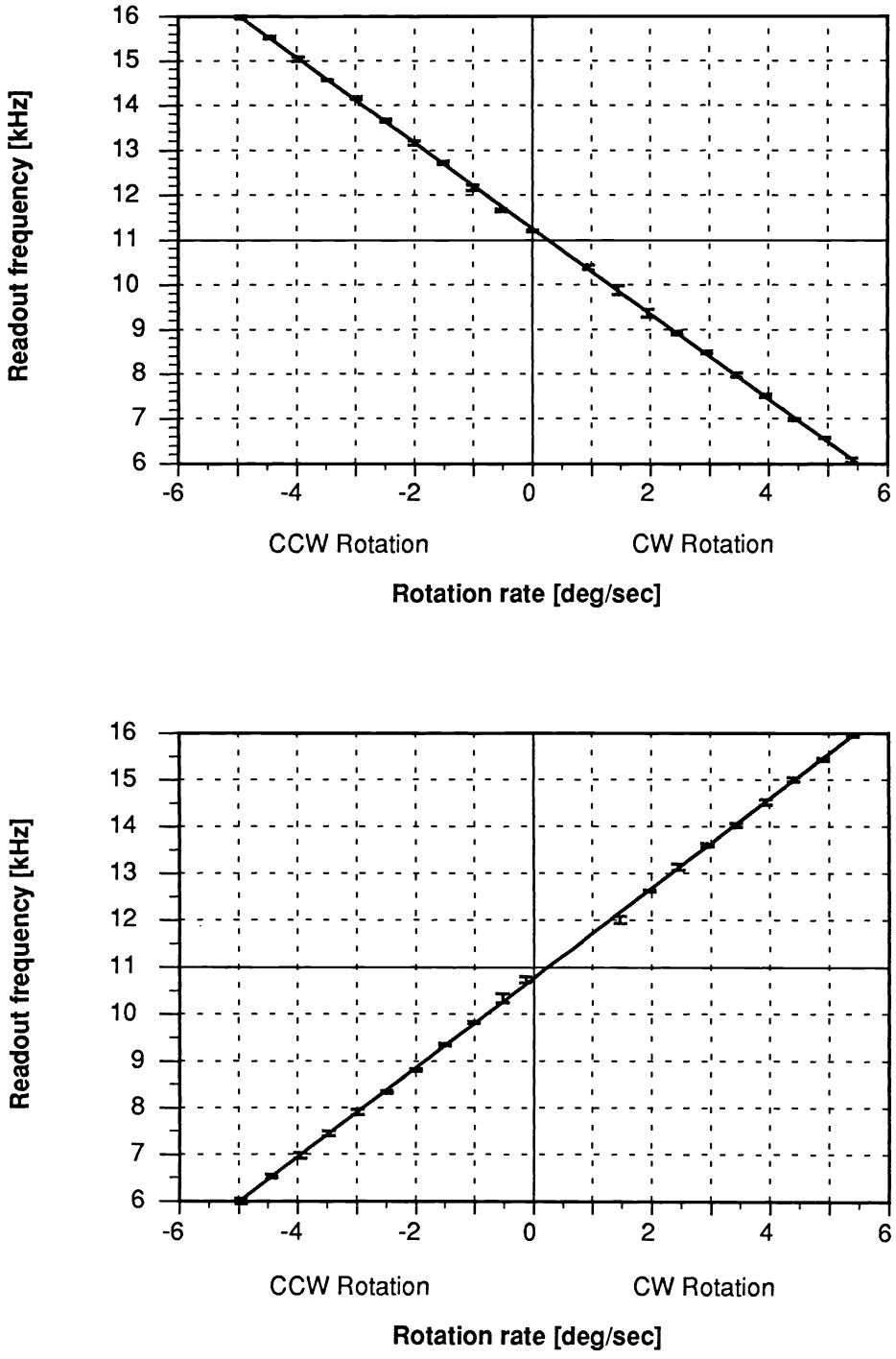

Figure 6. Measured curves of readout frequency f_{ro} vs rotation rate Ω_b, for phase delays in the $A(t)$ generator with a 180° difference. The push-pull phase modulation frequency used was 11 kHz.